Journal of Quantitative Spectroscopy & Radiative Transfer 111 (2010) 1289–1295

Contents lists available at ScienceDirect

Journal of Quantitative Spectroscopy & Radiative Transfer

journal homepage: www.elsevier.com/locate/jqsrt

An improved high-resolution solar reference spectrum for earth's atmosphere measurements in the ultraviolet, visible, and near infrared

K. Chance *, R.L. Kurucz

Harvard-Smithsonian Center for Astrophysics, Cambridge, MA 02138, USA

ARTICLE INFO

Article history:
Received 16 November 2009
Received in revised form
28 January 2010
Accepted 29 January 2010

Keywords:
Solar spectrum
Remote sensing
Atmospheric spectroscopy

ABSTRACT

We have developed an improved solar reference spectrum for use in the analysis of atmospheric spectra from vacuum wavelengths of 200.07 through 1000.99 nm. The spectrum is developed by combining high spectral resolution ground-based and balloon-based solar measurements with lower spectral resolution but higher accuracy irradiance information. The new reference spectrum replaces our previous reference spectrum, and its derivatives, for use in a number of physical applications for analysis of atmospheric spectra, including: wavelength calibration; determination of instrument transfer (slit) functions; Ring effect (Raman scattering) correction; and correction for spectral undersampling of atmospheric spectra, particularly those that are dilute in absorbers. The applicability includes measurements from the GOME, SCIAMACHY, OMI, and OMPS satellite instruments as well as aircraft-, balloon-, and ground-based measurements.

Published by Elsevier Ltd.

1. Introduction

Measurements of small absorptions in the Earth's atmosphere have enabled the quantitative determinations of many important atmospheric gases. For satellite-based measurements in the ultraviolet, visible, and near infrared, these include ozone (O_3, including profiles and tropospheric concentrations), nitrogen dioxide (NO_2), sulfur dioxide (SO_2), formaldehyde (HCHO), glyoxal (CHOCHO), bromine oxide (BrO), iodine oxide (IO), chlorine dioxide (OClO), and water vapor (H_2O). Analysis of atmospheric spectra to obtain amounts of these gases requires careful quantitative modeling and fitting of spectra, sometimes to precisions as small as several times 10^{-4} of the full-scale radiances over tens of nanometers (cf. Chance [1]). The algorithm physics required to obtain such precisions includes a number of applications of an independent solar reference spectrum, which is at substantially higher spectral resolution than the atmospheric measurements themselves, which are typically obtained at several tenths of a nanometer resolution. These applications, which are discussed in more detail in Section 4, include wavelength calibration, determination of instrument transfer, or slit, functions (ITFs), Ring effect correction, and correction for spectral undersampling of atmospheric spectra which are dilute in absorbers. Algorithms for a number of products from the Global Ozone Monitoring Experiment (GOME-1 and GOME-2), Scanning Imaging Absorption Spectrometer for Atmospheric Chartography (SCIAMACHY), Ozone Monitoring Experiment (OMI), and Ozone Mapping and Profiler Suite (OMPS) satellite instruments [2–6] have been developed using a previous version of the Smithsonian Astrophysical Observatory (SAO) reference spectrum [7]. The reference spectrum presented here is derived from the Fourier transform spectroscopy measurements of the Sun from 293.09 to 1627.02 vacuum nm using the McMath solar telescope at Kitt Peak National Observatory (Kurucz [8],

* Corresponding author.
E-mail address: Kchance@CfA.Harvard.edu (K. Chance).

0022-4073/$ - see front matter Published by Elsevier Ltd.
doi:10.1016/j.jqsrt.2010.01.036

hereafter the "KPNO spectrum"), and balloon-based measurements of the Sun using a grating spectrometer from 200.06 to 310.09 vacuum nm (Hall and Anderson, [9], hereafter the "AFGL spectrum").

The new solar reference spectrum presented here takes advantage of two improvements. First, the KPNO spectrum has now been recalibrated in intensity so that it agrees to within 1% at coarse spectral resolution with the lower spectral resolution reference spectrum developed by Thuillier et al. [10], which is now generally accepted as an intensity standard, and has absolute accuracy of 3.5–4% over the wavelength range addressed here. Second, there is now improved knowledge of spectral sampling [11], which is applied here to produce a fully *Nyquist sampled* reference spectrum [12] that may be resampled on any desired grid, e.g. for spectral comparison purposes, with negligible error.

2. Background

The original spectrum used for the present algorithm purposes [7] was from an earlier intensity analysis of the KPNO spectrum, combined with the AFGL spectrum. The KPNO spectrum was re-calibrated in wavelength using 4 O_2 lines [13], to an accuracy of better than 0.001 nm (perhaps much better). The intensities were used as is. The AFGL spectrum was re-checked for wavelength accuracy using 20 atomic lines [14,15], giving an accuracy of 0.003 nm (1σ). These intensities were also used as is. Each spectrum was then re-sampled at even 0.01 nm increments using a triangular filter of 0.02 nm full-width at half-maximum (FWHM). They were linearly merged together over the 300–305 nm range.

The resulting spectrum (sometimes referred to in the satellite literature as the "Kurucz spectrum," but referred to here as SAO96) has been used at the SAO and by a number of other research groups for implementing the algorithm physics for the GOME, SCIAMACHY, OMI, and OMPS satellite instruments. We have normally provided it over the 230–800 nm spectral region, although we have produced versions extending to beyond 1000 nm and also at higher spectral resolution (0.001 nm) for specialized purposes.

In 2000, as part of the OMPS instrument and algorithm development, SAO produced a version of the solar calibration spectrum with local radiometric calibration to renormalize the high-resolution spectrum to a lower-resolution spectrum of higher radiometric accuracy, derived from SOLSTICE and SUSIM [16] and the US Air Force LOWTRAN/ MODTRAN solar spectrum [17] locally, using a triangular band pass of selectable width (usually 2 nm). The spectrum was calculated from 235 to 1100 nm, with SOLSTICE/SUSIM used at shorter wavelengths and LOWTRAN/MODTRAN at longer wavelengths, with a linear merge from 405.6 to 410.6 nm. Recently, Dobber et al. [18] performed an analogous intensity re-calibration over the more limited OMI spectral range (250-550 nm). Following our approach and starting with the SAO96 spectrum, they use the composite spectrum of Thuillier et al. [19], which is derived from SOLSTICE and SOSP measurements, as the low-resolution radiometrically accurate intensity source to determine a derivative of the SAO96 solar reference spectrum over this range.

3. The SAO2010 solar reference spectrum

As a starting point, the spectra that made up the Kitt Peak Solar Flux Atlas [8] have been re-reduced by Kurucz to produce an accurate solar irradiance spectrum (http://kurucz.harvard.edu/sun/fluxatlas2005/). The scans were smoothed with a 3-point Gaussian and an approximate atmospheric model was determined for each observation. Large scale features produced by O_3 and the O_2–O_2 collision complex were computed and divided out. The telluric line spectrum was computed using HITRAN 2004 [20] and other line parameter data for H_2O, O_2, and CO_2. The line parameters were adjusted for an approximate match to the observed spectra. The solar continuum level was found by fitting a smooth curve to high points in the observed spectrum while comparing with the product of the computed solar spectrum times the computed telluric spectrum. The spectrum was normalized to the fitted continuum to produce a residual flux spectrum for each FTS scan. Those scans were divided by the computed telluric spectra to produce residual irradiance spectra (http://kurucz.harvard.edu/sun/IRRADIANCE2005/). Artifacts from wavelength mismatches, deep lines, etc, were removed by hand. Overlapping scans were fitted together to make a continuous spectrum. The resulting spectrum was matched in intensity to the Thuillier et al. spectrum corresponding to higher solar activity (March 29, 1992) [10], to better than 1% at 0.5 nm spectral resolution for much of the spectrum; note that there are some significant differences in individual features (including some noise features) at higher spectral resolution (http://kurucz.harvard.edu/sun/irradiance2005/irradthu.dat). This spectrum (hereafter "KPNO2010") is used from 300 nm longward. Fig. 1 compares KPNO2010, convolved with a triangular band pass of 0.5 nm FWHM, and the Thuillier et al. spectrum. The upper panel shows the two spectra. The middle panel shows relative differences (normalized to Ref. [10] at the 0.5 nm resolution. The lower panel compared the spectra at a triangular band pass of 20 nm FWHM. Agreement at this coarse resolution is at the 1% level or better, except for several disagreements at the 2% level at shorter wavelengths. Higher resolution disagreement is due mostly to noise in the Thuillier et al. measurements. As with SAO96, the shorter wavelength spectrum contributing to SAO2010 is taken from Hall and Anderson [9], used from 305 nm shortward, calibrated as in SAO96 (hereafter "AFGL").

The KPNO2010 spectrum is tested for wavelength accuracy against the ESA PtCrNe line lamp listing [21] (the irradiance spectrum is corrected for the solar gravitational redshift, 0.636 km s^{-1}, for the comparison). The agreement in line positions using 25 lines is accurate to 2.5×10^{-4} nm (1σ), where the line lamp accuracy is estimated at 0.002 cm^{-1}, corresponding to 2×10^{-5} nm at 300 nm and 2×10^{-4} nm at 1000 nm. The AFGL spectrum remains unchanged from SAO96, with 0.003 nm wavelength accuracy. Thus the overall absolute wavelength

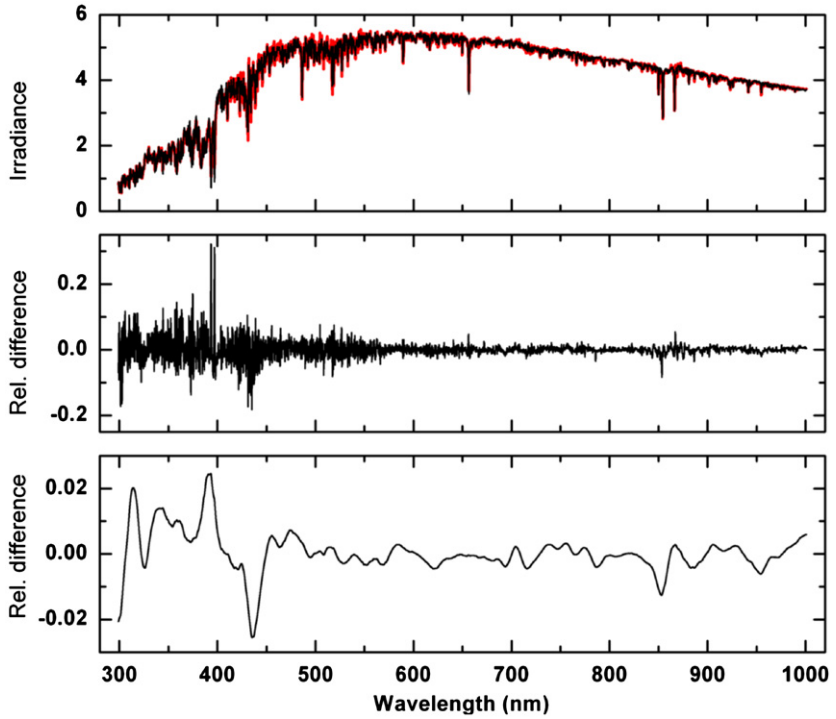

Fig. 1. Top panel: Thuillier et al. [10] and Kurucz 2010 solar irradiance spectra (10^{14} photons s^{-1} cm^{-2} nm^{-1}) at 0.5 nm FWHM triangular band pass. Middle panel: relative differences (Thuillier–Kurucz)/Thuillier. Lower panel: differences at 20 nm FWHM triangular band pass.

accuracy is $\leq 3.2\times10^{-4}$ nm (quadrature sum of position agreement and lamp line accuracy) above 305 nm and $\leq 3\times10^{-3}$ nm below 305 nm.

The KPNO2005 and AFGL spectra are each convolved to a Gaussian full-width at half-maximum (FWHM) of 0.04 nm and sampled to 0.01 nm, to avoid undersampling (sampling a Gaussian at 4 times the FWHM guarantees sampling error of less than 1 part in 10^7 [11]). The convolved spectra are then linearly tapered together from 300 to 305 nm. Fig. 2 shows the SAO2010 spectrum and its logarithm.

Fig. 3 is a comparison of SAO2010, SAO96, the Dobber et al. [18], and the Thuillier et al. [10] spectra over the range 305–600 nm (upper panel), and an expanded view from 305 to 400 nm, where much of the atmospheric trace gas fitting is performed (lower panel). This range is chosen because the Thuillier et al. spectrum completely guides the SAO2010 intensity above 305 nm and Dobber et al. only extends to 600 nm. The comparison is made at 1 nm FWHM, so that high-resolution structure does not obscure the relative intensity calibration. The most obvious discrepancies are with SAO96 from 305 to 330 nm, where O_3 structure was not fully removed. Unlike the SAO recalibration of the shorter wavelength portion of the spectrum with SOLSTICE/SUSIM for OMPS, the Hall and Anderson [9] spectrum was not recalibrated in intensity here. This is chiefly because we have concentrated on the recalibration of the KPNO spectrum, which covers the wavelength region where most applications to satellite measurements are performed. Thus, the intensities for the portion of SAO2010 shortward of 305 nm may be in substantial disagreement with both Thuillier et al. [8] and Dobber et al. [18] (by as much as 20%). This will be addressed more fully in the future using the calibration techniques developed for OMPS and the present KPNO recalibration, and will be updated at SAO as space-based solar irradiances [10,19] are improved.

In addition to a better intensity calibrated high-resolution spectrum, the procedure adapted here provides a better sampled spectrum for further use. It is now properly Nyquist sampled, unlike SAO96 and the Dobber et al. spectrum derived from it [18].[1]

4. Application in spectral data analysis

The applications summarized here rely most importantly on absolute wavelength calibration and on relative intensity calibration which maintains its precision over wavelength windows where atmospheric species (primarily gases) are analyzed. In particular, the corrections for Ring effect and spectral undersampling are normally included as parameters with adjustable intensities [1], since their relative contributions in an atmospheric spectrum depend quantitatively on atmospheric constituents

[1] Nyquist sampling, as described, e.g., in Goldman [12] is an ideal situation, even for Fourier transform spectrometers (due to complications from finite sampling times and detector integration circuitry). As a practical matter, we use the term here to apply to situations where residual sampling error [11] is negligible compared to measurement noise.

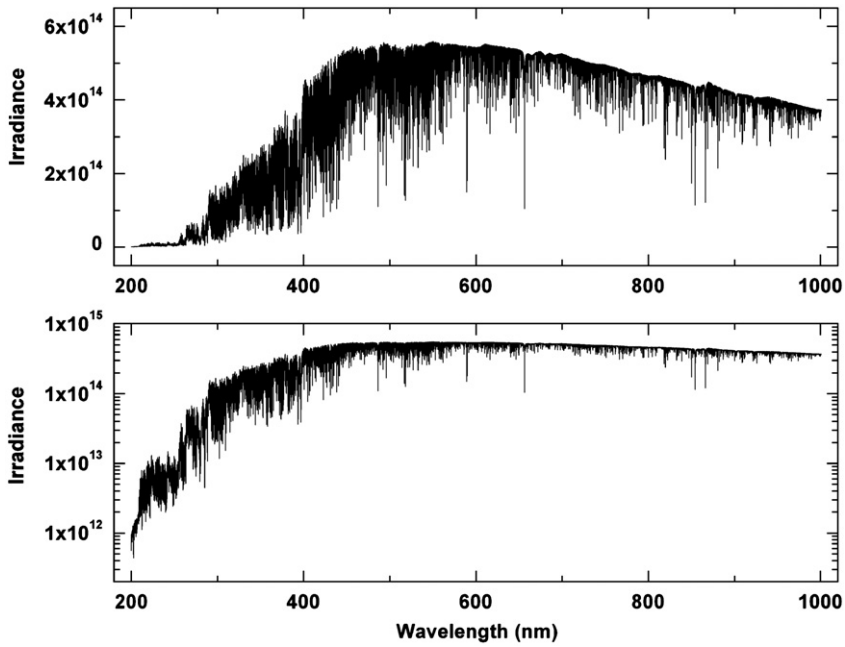

Fig. 2. Upper panel: the SAO2010 irradiance reference spectrum (photons s^{-1} cm^{-2} nm^{-1}). Lower panel: irradiance on a logarithmic scale.

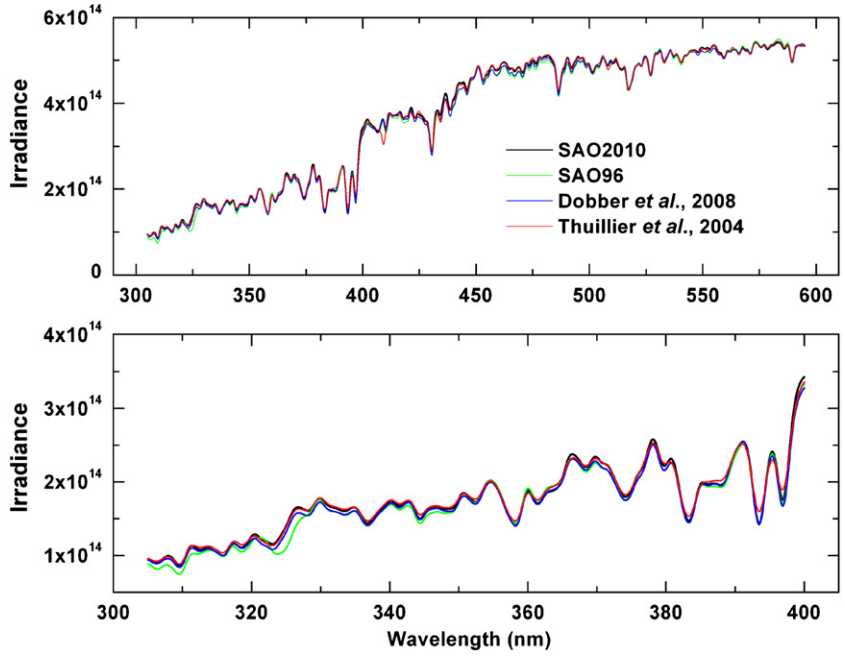

Fig. 3. Comparisons among irradiance spectra: the new SAO2010 spectrum, the SAO96 spectrum, the Dobber et al. [18] spectrum, and the extra-atmosphere Thuillier et al. [10] spectrum. Irradiances are in photons s^{-1} cm^{-2} nm^{-1}.

whose spectra vary at low spectral frequency, including aerosol and cloud content and surface albedo.

4.1. *Wavelength and ITF calibration*

Wavelength calibrations are performed using a cross-calibration procedure derived from the method developed for fitting galactic redshifts [22]. Initially, segments of two spectra were cross-correlated in Fourier transform space by transforming, multiplying the transforms, and back-transforming the result. First studies on GOME-1 data [23] employed the XCSAO task of the RVSAO radial velocity package developed at the SAO Telescope Data Center (http://tdc-www.harvard.edu/TDC.html) for the

Image Reduction and Analysis Facility (IRAF) [24]. Because of the astrophysical origin of the software, the resulting spectral shifts were given in $km\,s^{-1}$. Instrument transfer functions (slit widths) were initially implemented on an *ad hoc* basis. This method was then replaced by nonlinear least-squares fitting of spectral segments (wavelength windows), where slit function parameters (initially a Gaussian width, but extendable to arbitrary parameterized slit functions) may be varied in addition to wavelength shift [23]. (Other wavelength-dependent parameters, such as "squeeze"—compression or expansion of the wavelength scale may also be fitted, but are not normally required for typical wavelength windows.) The capability to use the SAO96 spectrum and our cross-correlation approach to calibrate GOME-1 in wavelength to better than 0.01 detector pixel (0.002 nm accuracy below and 0.001 nm precision – accuracy is limited by the 0.003 nm absolute wavelength knowledge – above 290 nm) has been confirmed by van Geffen and van Oss [25].

Wavelength calibration based on this method has now been implemented in operational 0–1 processing code for the GOME, SCIAMACHY, OMI, and OMPS satellite instruments. Typically, a number of wavelength windows are fitted for each detector array ("channel") using this method, and the results are then tied together using a low-order function (usually a polynomial) to give the calibration for the entire channel (cf. [25,26]). It is then common to improve this calibration during 0–1 processing by fitting over the exact wavelength window being used for determination of atmospheric contents [1].

4.2. Ring effect correction

The "Ring effect" (Grainger and Ring [27]) is the manifestation in atmospheric spectra that Rayleigh scattering is partially inelastic. The inelastic component is Raman scattering by air molecules, predominantly rotational Raman scattering. The inelastic component varies from 4.0% to 3.4% of the total scattering over the prime atmospheric trace gas wavelength fitting region of 280–1000 nm [7,28]. Thus, to first order, the correction for the Ring effect in atmospheric spectra is simply the convolution of the irradiance with the spectrum of Raman scattering by air molecules, where the cross sections for

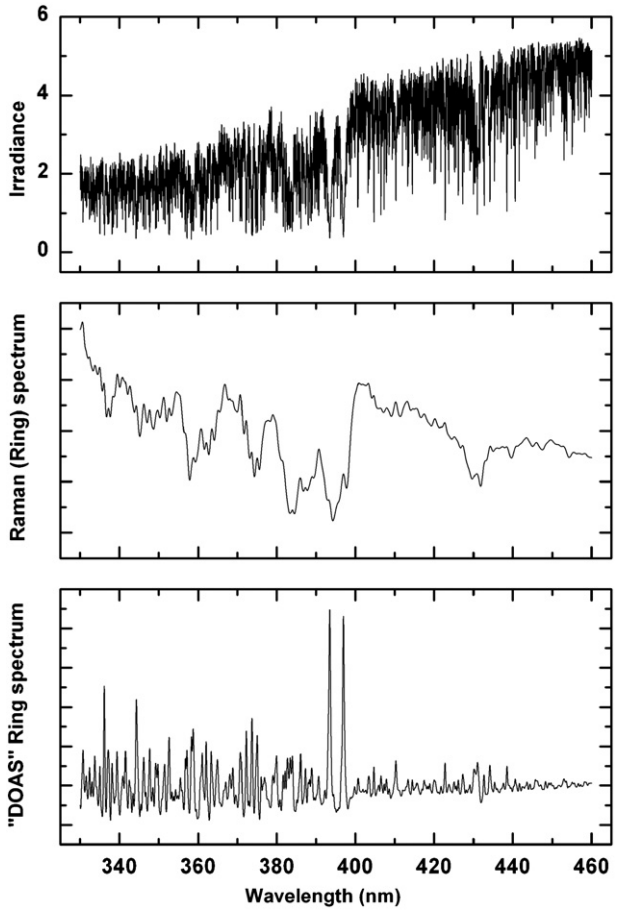

Fig. 4. Top panel: the SAO irradiance spectrum (10^{14} photons $s^{-1}\,cm^{-2}\,nm^{-1}$) over the wavelength range where the molecules NO_2, HCHO, CHOCHO, BrO, OClO, and IO are measured in atmospheric spectra. Middle panel: the Ring spectrum, i.e., the inelastic (Raman) component of Rayleigh scattering. Lower panel: the DOAS Ring correction spectrum, which is a high pass filtered version of (Ring/irradiance).

the dominant rotational Raman component are given by Chance and Spurr [7]. SAO provides Ring effect correction spectra and software based on these cross sections and SAO solar reference spectra (http://www.cfa.harvard.edu/atmosphere). Previous calculations, based on SAO96, are now replaced with SAO2010. The software includes the provision for correcting Ring effect scattering by interferences from molecular absorption, e.g., by O_3, to arbitrary order. Fig. 4 shows the SAO2010 solar reference spectrum for the portion of the UV/visible where many gases are measured in the atmospheric spectrum (top panel). The middle panel shows the Ring corrections spectrum, calculated as the convolution of SAO2010 with the spectrum of rotational Raman scattering by air molecules [7]. The lower panel is a high-pass filtered version of the ratio of the Raman spectrum to the irradiance, appropriate for use in the DOAS variant of spectral fitting, wherein a high-pass filtered logarithm of the ratio of the radiance to the irradiance is fitted rather than fitting the radiance or its logarithm directly [29]. The middle and lower panels are convolved with a Gaussian of 0.2 nm FWHM resolution, typical of atmospheric spectrometers.

4.3. Undersampling correction

Initial attempts to perform spectral fitting on satellite-based atmospheric spectra in the UV/visible suffered from substantial systematic fitting residuals. It was demonstrated that these are predominantly due to undersampling in the spectra [1]. The failure to Nyquist sample the atmospheric spectra by UV/visible satellite spectrometers to date has meant that the interpolation necessary to construct synthetic radiances from the satellite-measured solar irradiances as part of the fitting process produces significant systematic spectral structures: irradiances are substantially shifted in wavelength from radiances, chiefly from the Doppler shift due to the measurement geometry, but also partly due to variations in instrument temperature. Spectra which are not Nyquist sampled cannot be re-sampled in wavelength without introducing spurious features due to spectral aliasing. The structures introduced by aliasing can be largely corrected in the case where atmospheric absorptions are optically thin by calculating an undersampling correction using an independent, higher resolution, solar reference spectrum [1,11,30].

4.4. Testing on GOME-1 spectra

Spectral fitting using the SAO96 and SAO2010 irradiances are compared for an orbit of GOME-1 spectra, analyzing for bromine oxide (BrO) from 344.6 to 359.0 nm and for ozone (O_3) from 324.9 to 335.1 nm. The use of SAO2010 makes negligible difference in uncertainties for irradiance and radiance wavelength calibrations, slit widths, and slant column uncertainties (which include undersampling correction) for BrO. For O_3, the uncertainties in irradiance wavelength calibration and slit width improve by about a factor of two. Uncertainties in radiance wavelength calibration and slant columns show negligible difference. This confirms that SAO96 is a very good reference spectrum, except that correction for ozone absorption, as can be seen in Fig. 3, is incomplete. The improvement when using SAO2010 for these purposes is modest.

5. Conclusions

We have developed an improved solar reference spectrum, SAO2010.solref, for use in the analysis of ultraviolet, visible, and near-infrared atmospheric radiance spectra. The spectral range is 200.07–1000.99 nm, the resolution is 0.04 nm FWHM, sampled at 0.01 nm, with absolute radiometric intensity accuracy better than 5% at wavelengths longer than 305 nm, determined by matching to the Thuillier et al. [10] spectrum, which has absolute accuracy of 3.5–4% over the wavelength range addressed here. The absolute vacuum wavelength accuracy is $\leq 3.2\times10^{-4}$ nm above and $\leq 3\times10^{-3}$ nm below 305 nm. SAO2010.solref is available for general use at http://www.cfa.harvard.edu/atmosphere. Applications using the previous SAO96 spectrum and its derivatives should migrate to this new reference spectrum. In the future, we hope that it will be possible to obtain space-based Fourier transform solar spectra at sufficient spectral resolution and wavelength coverage to replace the compound reference spectrum developed here for even more accurate analysis of Earth radiance spectra.

Acknowledgements

We congratulate Dr. Laurence Rothman on the occasion of his 70th birthday. We gratefully acknowledge substantial contributions to this work by G.P. Anderson and the late L.A. Hall and also note with sadness the recent passing of J. Brault, whose genius in Fourier transform spectroscopy will be sorely missed. Input from the anonymous reviewers made this paper stronger and more useful. This research has been supported by NASA and the Smithsonian Institution.

References

[1] Chance K. Analysis of BrO measurements from the Global Ozone Monitoring Experiment. Geophys Res Lett 2008;25:3335–8.
[2] European Space Agency. The GOME Users Manual. European Space Agency Publication SP-1182, F. Bednarz, ed. European Space Agency, Noordwijk, The Netherlands, 1995.
[3] Callies J, Corpaccioli E, Eisinger M, Lefebvre A, Munro R, Perez-Albinana A, et al. GOME-2 ozone instrument onboard the European METOP satellites. Proc SPIE Weather Environ Satell 2004;5549:60–70.
[4] Burrows JP, Chance KV. Scanning imaging absorption spectrometer for atmospheric chartography. Proc SPIE Future Eur Jpn Remote Sensing Sensors Prog 1991;1490:146–54.
[5] Levelt PF, van den Oord GHJ, Dobber MR, Malkki A, de Vries J, Stammes P, et al. The ozone monitoring instrument. IEEE Trans Geosci Remote Sensing 2006;44:1093–101, doi:10.1109/TGRS.2006.872333.
[6] Flynn LE, Seftor CJ, Larsen JC, Xu P. The Ozone Mapping and Profiler Suite. In: Qu JJ, Gao W, Kafatos M, Murphy RE, Salomonson VV, editors. Earth science satellite remote sensing, vol. 1: science and

instruments Berlin, Heidelberg: Springer; 2007. p. 279–96, doi:10.1007/978-3-540-37293-6.
[7] Chance K, Spurr RJD. Ring effect studies: Rayleigh scattering, including molecular parameters for rotational Raman scattering, and the Fraunhofer spectrum. Appl Opt 1997;36:5224–30.
[8] Kurucz RL, Furenlid I, Brault J, Testerman L. Solar flux atlas from 296 to 1300 nm. National Solar Observatory, Sunspot, New Mexico, 1984.
[9] Hall LA, Anderson GP. High-resolution solar spectrum between 200 and 3100 Å. J Geophys Res 1991;96:12927–31.
[10] Thuillier G, Floyd L, Woods TN, Cebula R, Hilsenrath E, Hersé M, et al. Solar irradiance reference spectra. In: Pap JM, editor. Solar variability and its effect on the earth's atmosphere and climate system. AGU: Washington, DC; 2004. p. 171–94.
[11] Chance K, Kurosu TP, Sioris CE. Undersampling correction for array-detector based satellite spectrometers. Appl Opt 2005;44: 1296–304.
[12] Goldman S. Information theory. New York: Prentice-Hall; 1953.
[13] Newnham DA, Ballard J. Visible absorption cross sections and integrated absorption intensities of molecular oxygen (O_2 and O_4). J Geophys Res 1998;103:28,801–816, doi:10.1029/98JD02799.
[14] Moore CE. An ultraviolet multiplet table. NBS Circular 488, Section I. US Government Printing Office, Washington, DC, 1950.
[15] Moore CE. An ultraviolet multiplet table. NBS Circular 488, Section II. US Government Printing Office, Washington, DC, 1952.
[16] Woods TN, Prinz DK, Rottman GJ, London J, Crane PC, Cebula RP, et al. Validation of the UARS solar ultraviolet irradiances: comparison with the ATLAS I and 2 measurements. J Geophys Res 1996;101:9541–69.
[17] Kneizys FX, Shettle EP, Abreu LW, Chetwynd JH, Anderson GP, Anderson WO, et al. Users guide to LOWTRAN 7. AFGL-TR-0177. US Air Force Geophysics Laboratory, Hanscom Air Force Base, MA, 1988.
[18] Dobber M, Voors R, Dirksen R, Kleipool Q, Levelt P. The high-resolution solar reference spectrum between 250 and 550 nm and its application to measurements with the Ozone Monitoring Instrument. Sol Phys 2008;249:281–91, doi:10.1007/s11207-008-9187-7.
[19] Thuillier G, Hersé M, Labs D, Foujols T, Peetermans W, Gillotay D, et al. The Solar spectral irradiance from 200 to 2400 nm as measured by the SOLSPEC spectrometer from the ATLAS and EURECA missions. Sol Phys 2003;214:1–22.
[20] Rothman LS, Jacquemart D, Barbe A, Benner DC, Birk M, Brown LS, et al. The HITRAN 2004 molecular spectroscopic database. JQSRT 2005;96:139–204.
[21] Murray JE. Atlas of the spectrum of a platinum/chromium/neon hollow-cathode reference lamp in the region 240–790 nm, ESA Report, European Space Agency, 1994.
[22] Tonry J, Davis M. A survey of galaxy redshifts. I—Data reduction techniques. Astron J 1979;84:1511–25.
[23] Caspar C, Chance K. GOME wavelength calibration using solar and atmospheric spectra. In: Guyenne T-D, Danesy D, editors. Proceedings of the third ERS symposium on space at the service of our environment. European Space Agency publication SP-414, ISBN 92-9092-656-2, 1997. p. 609–4.
[24] Kurtz MJ, Mink DJ, Wyatt WF, Fabricant DG, Torres G, Kriss GA, et al. XCSAO: A radial velocity package for the IRAF environment. In Worrall DM, C. Biemesderfer C, Barnes J, editors. Astronomical data analysis software and systems I, ASP Conference Series, Vol. 25, 1992. p. 432–8.
[25] van Geffen JHGM, van Oss RF. Wavelength calibration of spectra measured by the Global Ozone Monitoring Experiment by use of a high-resolution reference spectrum. Appl Opt 2003;42: 2739–53.
[26] NASA, OMI algorithm theoretical basis document volume 1: OMI Instrument Description and Level 1B Product. Levelt PF editor, 2002. 〈http://eospso.gsfc.nasa.gov/eos_homepage/for_scientists/atbd/〉.
[27] Grainger JF, Ring J. Anomalous Fraunhofer line profiles. Nature 1962;193:762.
[28] Bates DR. Rayleigh scattering by air. Planet Space Sci 1984;32: 785–90.
[29] Platt U, Perner D. Measurements of atmospheric trace gases by long path differential UV/visible absorption spectroscopy. In: Killinger DA, Mooradien A, editors. Optical and laser remote sensing. New York: Springer Verlag; 1983. p. 95–105.
[30] Slijkhuis S, von Bargen A, Thomas W, Chance K. Calculation of undersampling correction spectra for DOAS spectral fitting. Proceedings of the European symposium on atmospheric measurements from space, 1999. p. 563–9.